Modeling of Bubble Growth in Nucleate Flow Boiling Using OpenFOAM

Anuraj R S, Jayakumar J S
Dept. of Mechanical Engineering
Amrita Vishwa Vidyapeetham, Amritapuri Kollam, India
anurajrajan002@gmail.com
jsjayan@am.amrita.edu

***Abstract*—Numerical modeling of growth of a single bubble in nucleate flow boiling is presented in this paper. The modeling is done using the open-source CFD software OpenFOAM. The bulk fluid velocities used in the current study are 0.076 m/s and 0.1 m/s. A flow domain is chosen such that the bulk fluid temperature is at its saturation and the walls are at a higher temperature than the bulk fluid temperature. OpenFOAM has inbuilt solvers for solving various problems. First of all, a base solver is selected which deals with two-phase flow problems. Continuity, momentum and energy equations are solved numerically and the interface is captured by volume-of-fluid (VOF) method. The interfacial forces such as drag and lift which act on the bubble are also included. Thus a new solver namely *bubbleEvapTempFoam* is created and compiled for the current investigation. Initially a bubble is set up with a given diameter using the *setFieldsDict* dictionary. The boundary conditions such as pressure, velocity of fluid, velocity of vapor, temperature and void fraction are provided in the *0* dictionary. These conditions are applied at the internal bulk fluid and the boundaries such as inlet, outlet and walls. Output at various instances are viewed by using the post processing utility *paraView*. Bubble diameter as a function of time are estimated from the void fraction contours and is plotted. Bubble growth for different initial bubble diameters are also studied. The results are compared with data from previous literatures.**

***Keywords*—Bubble growth, nucleate boiling, OpenFOAM, CFD, heat transfer**

I. INTRODUCTION

Boiling heat transfer is used in wide range of applications. Some common areas of application include heat exchangers, nuclear reactors, etc. Among various regimes of boiling, the nucleate boiling is efficient in heat removal. There are various research efforts to understand the physics of boiling. Due to its high cooling effectiveness, it is employed in many industrial and engineering applications. The boiling mechanism provides constant wall temperature from the saturation state up to critical heat flux. Nucleate boiling is characterised by the evolution and growth of bubbles. The vapour bubbles are formed at discrete sites in nucleate boiling. The frequency and nucleation site density increases with the wall superheat. For space applications, this mode of heat removal is found to be very effective. Thus the study of bubble characteristics has become important.

A physical model for the dynamics of vapour bubbles were presented by Meister [1]. The model was applicable for bubbles generated in channels with heated walls. The correlations used in this model for bubble lifetime and bubble size were derived from predictions of vapour components in heated channels with subcooled inlet flow. Their results of bubble size, bubble lifetime and recondensation rate were found to be in good agreement with previous experimental results. In this, the bubble behaviour in subcooled flow is properly modelled whereas there are deviations in areas of high fluid subcooling. The liquid inertia is neglected since it is significant only for a short period in the initial growth. The heat transfer due to microlayer was found to be varying with bubble lifetime but not with time. The heat flow over the microlayer and the separated layer was found to be hardly distinguishable for a limited attachment period. In bubble detachment under forced flow conditions along heated channel, the bubble detaches from the surface when the drag and buoyant forces overcome the adhesive forces between the bubble and wall. Different parameters such as bubble radius versus time, thermal boundary layer thickness versus subcooling, fluid velocity and heat flux density were plotted.

The nucleate boiling regime for water circulating in a closed loop at atmospheric pressure was experimentally investigated by Maurus and Sattelmayer [2]. To study the characteristics of the bubble and fluid, the experiment was done on a horizontally oriented rectangular channel test section. One side of the test section was fabricated so as to have good optical access while the other side is made of copper. A high resolution digital camera and high-speed cinematography were used to record the bubble behaviour. The bubble size, bubble lifetime and bubble waiting time were evaluated by analysing the images of bubbles. A statistical analysis was performed and a distribution function was derived since a large number of bubbles were evolved during the process. Particle image velocimetry (PIV) was used to characterise the fluid velocity for single phase flow and subcooled flow boiling conditions. The increase in number of bubbles cause increase in resistance to fluid flow. The impact was found to be more in the bubbly region. Also the ratio of averaged phase boundary velocity and averaged fluid velocity was evaluated for the bubbly region.

A three dimensional numerical simulation of dynamics of single bubble was done by Li and Dhir [3]. In this the bubble shape is not approximated. The bulk fluid velocities investigated in this are 0.076 to 0.23 m/s. The surface orientation with the vertical was varied as 30, 45 and 60 degree. The gravity levels were varied from $0.0001g$ to $1.0g$, where g is the acceleration due to gravity. The continuity, momentum and energy equations were solved by finite difference method and level set method is used for interface capturing. The effect of heat transfer within microlayer and microlayer evaporation were included in the model. The numerical results were compared with experimental data. Bubble sliding prior to lift-off was well predicted. The results showed the effect of bulk fluid velocity, heater surface orientation and gravity on the bubble characteristics. As the bulk fluid velocity increases, the bubble lift-off diameter was found to decrease and with the decrease in component of gravity normal to the surface the lift-off diameter is found to increase. The effect of gravity on bubble lift-off diameter is weakened as the flow velocity is increased. The bubble lift-off diameter and growth period appears to have not at all affected by the magnitude of gravity for the flow velocity of 0.23 m/s.

The bubble lift-off diameter in subcooled flow was studied by Khanlou et al. [4] using AFL fire CFD software. A study was conducted on the scaled upward channel of a Boiling Water Reactor (BWR) to predict the bubble lift-off diameter. The numerical results were compared with experimental observation. To predict the bubble lift-off size, a force balance analysis was done on the growing bubble. The forced subcooled flow boiling experiment was done using a vertically upward annular channel with water as working fluid. The experiments were done at atmospheric pressure with inlet temperature ranging from 80 to 98.5 ºC and the inlet velocity ranging from 0.487 to 0.939 m/s. A digital camera was used to capture the images of growing bubbles and the images were analysed by using Matlab image processing toolkit. The results showed that the lift-off diameter increases with inlet temperature.

The nucleation and growth of bubble in a Newtonian fluid was studied by Naber et al. [5]. The analytical model developed was compared with classical models. The new model developed allows study of bubble nucleation, growth and coalescence. In this, a complete foaming process was simulated in a square domain with side length 500mm which is filled with 70/30 liquid-gas mixture and the fluid velocity assumed to be zero. At all grid points, a random disturbance was imposed and the gas concentration is varied from 25% to 35%. The bubbles form due to inhomogeneity in the domain and subsequently the bubbles grow. It was seen that the bubbles merge to form larger bubbles. The bubble departure frequency was investigated by Situ et al. [6] by considering a three-dimensional two-fluid model coupled with population balance equation. The bubbly flows were predicted with the CFX MUltiple-SIze-Group (MUSIG) model with the presence of heat and mass transfer processes, particularly in subcooled boiling flows at low pressures. The results indicated that the higher the departure frequency, the lower the wall temperature and thus the nucleation site density. The curves of the void fraction were found to decrease in both axial and radial cases with the increase in departure frequency.

In the present study, the growth of a vapour bubble in nucleate flow boiling is modelled using OpenFOAM. The interface capturing is done using the VOF method. For modelling bubble growth, a base solver called *bubbleFoam* is selected. The solver is modified by including energy equation and adding source term to the continuity equation. Also interfacial forces such as drag and lift are included in the new solver. It is then compiled to develop the new solver called *bubbleEvapTempFoam*, which is used for modelling the bubble growth. The solver is validated with results from available literature.

II. Description of the Problem

Nucleate boiling is characterised by the evolution and growth of bubbles. It is a complicated process due to the behaviour of the vapour bubbles and the high heat flux rates. Understanding the behaviour of the bubbles is important in understanding the nucleate boiling process. The growth of bubbles depends on the amount of heat absorbed by the fluid. The bubbles originate at the cavities on the solid surface where the vapour or non-condensable gases are trapped. Bubbles are formed when the walls are at a temperature higher than the saturation temperature and the local fluid temperature is at its saturation state. When the temperature of the wall becomes greater than the saturation temperature of the fluid, active nucleate sites are formed and bubbles evolve. Fig.1 shows the growth of vapour bubble in a saturated fluid. In the current work, the growth of a vapour bubble with specific initial diameter is presented. The fluid is at its saturation temperature and the walls are maintained at a temperature

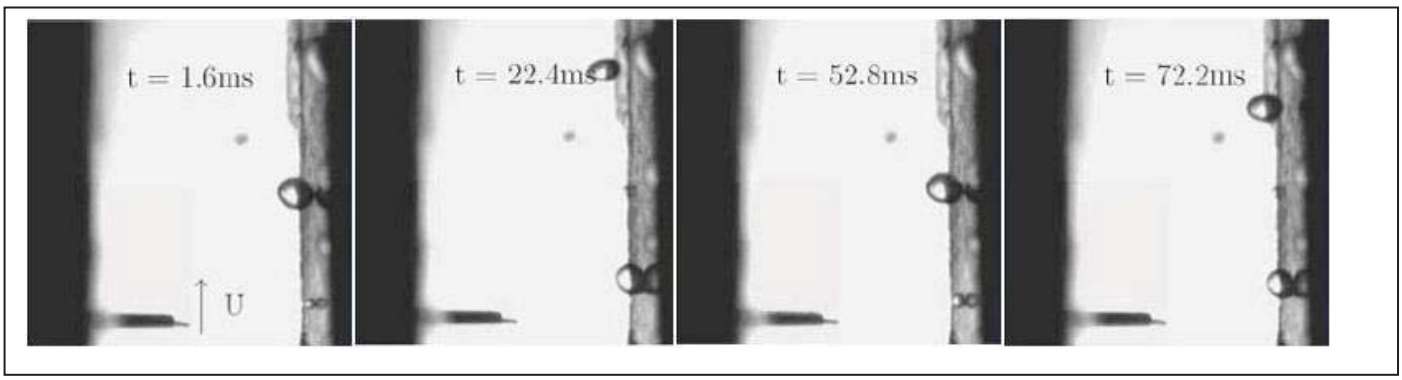

Fig.1 Bubble growth in nucleate flow boiling (Li and Dhir [3])

higher than the bulk fluid temperature.

III. OUTLINE OF THE WORK

In nucleate boiling, the heat absorbed by the fluid is characterised by the bubble growth. The bubble growth is the deciding factor in the heat and mass transferred in a nucleate boiling phenomenon. The governing equations are converted into OpenFOAM framework and added to a pre-existing base solver called *bubbleFoam* to form a new solver *bubbleEvapTempFoam*. Here VOF method is used to capture the liquid-vapour interface. The development of the new solver is shown in Fig. 2. The new solver is then used to solve the governing equations of the required computational domain. The case directory is then formed which includes various dictionaries to form the computational domain, to give the boundary conditions, to provide the discretisation schemes, etc. Fig. 3 shows the case structure of the current problem.

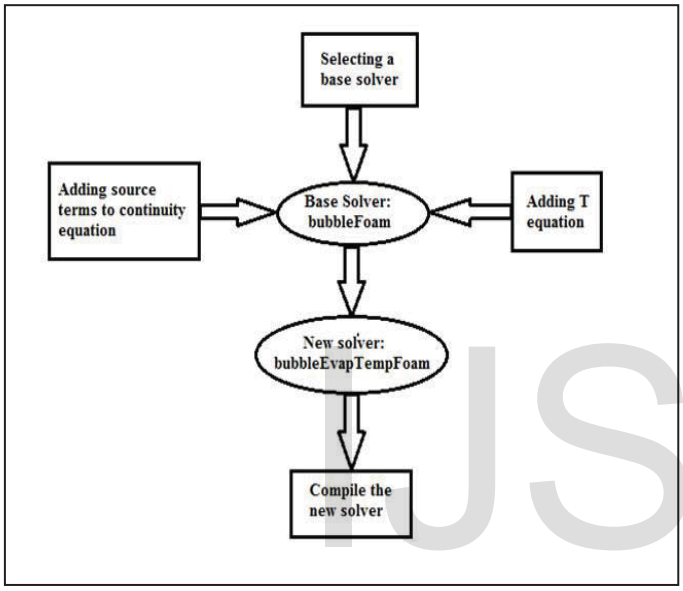

Fig.2 Development of *bubbleEvapTempFoam*

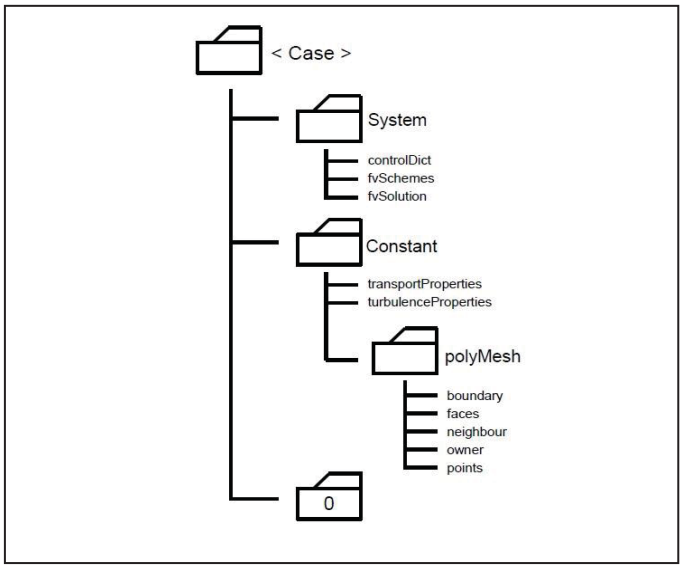

Fig.3 Case directory structure

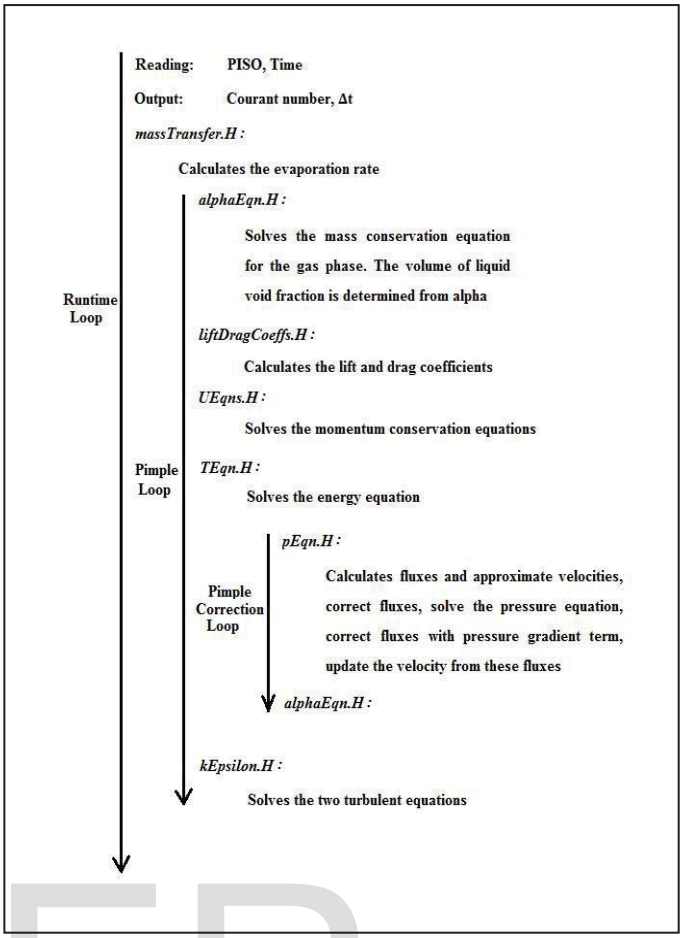

Fig.4 *bubbleEvapTempFoam* working loop

IV. NUMERICAL METHODOLOGY

A. Interface Tracking with VOF

Several methods are available to simulate two-phase flows. In this work, VOF method is used to capture a moving interface. The volume fraction α_i which is the partial volume of phase i to the total volume is utilised in this method. This method utilise the fact that the sum of volume fractions of all phases must be unity. Thus only (N-1) volume fractions are needed to describe N different phases. The volume fraction α is defined by:

$$\alpha = \frac{V}{V_{cell}} \quad (1)$$

The value of alpha varies from zero for vapour phase to one for liquid phase. The cells at the liquid vapour interface will have values between zero and one.

B. Governing Equations

The governing equations relating to the problem are implemented in OpenFOAM framework. The governing equations are the conservation, momentum and energy equations. Here, the continuous phase is taken as liquid and the dispersed phase is the vapour phase.

1) Continuity equation:

$$\frac{\partial \alpha_k}{\partial t} + \nabla.(\alpha_k U_k) = \frac{\Gamma_{ki} - \Gamma_{ik}}{\rho_k} \quad (2)$$

where *k* denotes the phases and can be *l* or *g* (liquid or gas) and *i* is the non-*k* phase. *α*, *ρ* and *U* represent the phase fraction, density and velocity respectively. Γ_{gl} corresponds to the evaporation rate and Γ_{lg} corresponds to the condensation rate. Here we are not taking into account the condensation as the temperature is always assumed to be greater than the saturation temperature. The continuity equation is solved for only one phase as the void fractions of both the phases are related as:

$$\alpha_l = 1 - \alpha_g \quad (3)$$

2) Momentum equation of phase k:

$$\frac{\partial \alpha_k U_k}{\partial t} + \nabla.(\alpha_k U_k U_k) = -\nabla.\left(\alpha_k (R_k + R_k^t)\right) - \frac{\alpha_k}{\rho_k}\nabla p + \alpha_k g + \frac{M_k}{\rho_k} + \frac{\Gamma_{ki} U_i - \Gamma_{ik} U_k}{\rho_k} \quad (4)$$

The turbulent stress tensor is given by:

$$R_k^{eff} = R_k + R_k^t = -(\nu_k + \nu_k^t)\left(\nabla U_k + (\nabla U_k)^T - \frac{2}{3} I \nabla. U_k\right) + \frac{2}{3} I k_k \quad (5)$$

Here, *υ* is the kinematic viscosity and *k* is the turbulent kinetic energy.

3) Energy equation:

The energy conservation equation is given in terms of specific enthalpy.

$$\frac{\partial((1-\alpha) i_l)}{\partial t} + \nabla.\left((1-\alpha) i_l U_l\right) = \frac{\Gamma_{lg} i_{g,sat} - \Gamma_{gl} i_l}{\rho_l} \quad (6)$$

Here *i* is the specific enthalpy.

C. Evaporation Rate

The evaporation rate is added mainly in the continuity equation as a source term. The evaporation rate is given by:

$$\Gamma_{gl} = \frac{q_w^{e''}}{i_{g,sat} - i_l} A_w''' = \frac{\pi}{6} d_w^3 \rho_v f N'' A_w \quad (7)$$

where,

$$A_w = \pi N'' d_w^2 \quad (8)$$

Here, d_w is written in terms of saturation temperature and liquid temperature.

$$d_w = 1.4 \times 10^{-6} exp\left(-\frac{T_{sat} - T_l}{45}\right) \quad (9)$$

The detachment frequency and nucleation site density are given by:

$$f = \sqrt{\frac{3}{4}\frac{(\rho_l - \rho_g) g}{\rho_l d_w}} \quad (10)$$

$$N'' = [210(T_w - T_{sat})]^{1.805} \quad (11)$$

D. Interfacial Forces

There are various forces which act on the bubble as a result of the fluid surrounding it. These interfacial forces include drag and lift forces. These forces are included in the solver and the governing equations are solved accordingly.

1) Drag force:

$$M_g^D = -\frac{3}{4}\frac{C_D}{D_S}\rho_l \alpha \|U_g - U_l\|(U_g - U_l) \quad (12)$$

where D_S is the Sauter diameter and C_D is given by:

$$C_D = max\left(24\frac{1 + 0.15 Re_b^{0.687}}{Re_b}, 0.44\right) \quad (13)$$

Re_b is the bubble Reynolds number given by:

$$Re_b = \frac{\rho_l \|U_g - U_l\| D_S}{\mu_m} \quad (14)$$

$$\mu_m = \mu_l\left(1 - \frac{\alpha}{\alpha_{max}}\right)^{-2.5\alpha_{max}\mu^*} \quad (15)$$

where, *μ* is the dynamic viscosity

Here α_{max} is the void fraction at maximum packing whose value is 0.52 and μ^* is the dimensionless viscosity given by:

$$\mu^* = \frac{\mu_g + 0.4\mu_l}{\mu_g + \mu_l} \quad (16)$$

2) Lift force:

$$M_g^L = C_L \rho_l \alpha (U_g - U_l) \wedge (\nabla \wedge U_l) \quad (17)$$

Here the lift coefficient C_L is given by:

$$C_L = \begin{cases} \min[0.288 \tanh(0.121 Re_b), f(Eo_d)], if\ Eo_d < 4 \\ f(Eo_d), if\ 4 \le Eo_d \le 10 \\ -0.27, if\ Eo_d > 10 \end{cases} \quad (18)$$

$$f(Eo_d) = 0.001509 Eo_d^3 - 0.0159 Eo_d^2 - 0.0204 Eo_d + 0.474 \quad (19)$$

Here Eo_d is the maximum horizontal dimension for the bubble. d_h is calculated accordingly.

$$Re_b = \frac{\|U_g - U_l\| D_S}{\nu_l} \quad (20)$$

$$d_h = D_S(1 + 0.163 Eo^{0.757})^{\frac{1}{3}} \quad (21)$$

$$Eo = \frac{g(\rho_l - \rho_g) D_S^2}{\sigma} \quad (22)$$

$$Eo_d = \frac{g(\rho_l - \rho_g)d_h^2}{\sigma} \quad (23)$$

The working loop of the solver *bubbleEvapTempFoam* is shown in Fig. 4. In the solver, the outer loop is the Runtime Loop where the PISO loop is executed and the time is read. The output gives the Courant number and Δt and the feasibility of the process is checked. The header file *massTransfer.H* will compute the evaporation rate of the liquid according to Eqn. 7. Then the program enters the Pimple Loop where the continuity, momentum and energy equations are solved. First, the *alphaEqn.H* solves the continuity equation according to Eqn. 2 which computes alpha. Then *liftDragCoeffs.H* calculates the lift and drag forces according to Eqn. 12 and 17. The momentum equation in Eqn. 4 is solved by *UEqns.H* and the energy equation in Eqn. 6 by *TEqn.H*. The Pimple Correction Loop calculates and approximate the fluxes, solves the pressure equation, correct the fluxes and update the velocity from these corrected fluxes. The *alphaEqn.H* is executed again in the Pimple Correction Loop. After that, the turbulent equations are solved by using *kEpsilon.H*.

V. Simulation Procedure

The geometry and mesh are created in the three-dimensional cartesian coordinate by using a utility called *blockMeshDict*. The dimensions of the domain are 0.0015×0.003×0.0015 m^3. Meshing is done such that it is divided into 25×75×25 cells. The geomety and mesh are shown in Fig. 5 and 6 respectively.

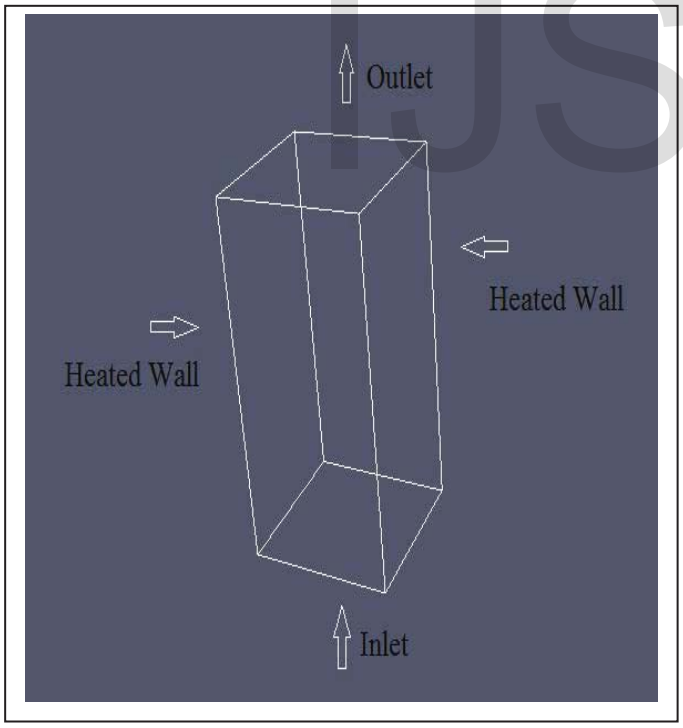

Fig. 5 Geometry of the domain

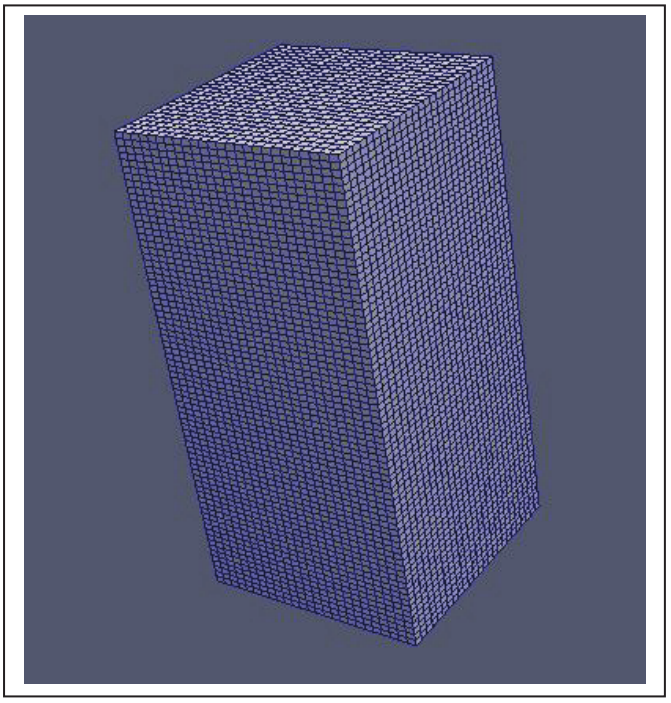

Fig.6 Meshed geometry

The initial and boundary conditions such as the temperature and velocity are given in the *0* directory. The initial bubble is set up in the fluid by using the *setFieldsDict* dictionary. Fig. 7 shows the initial bubble of diameter 0.5mm.

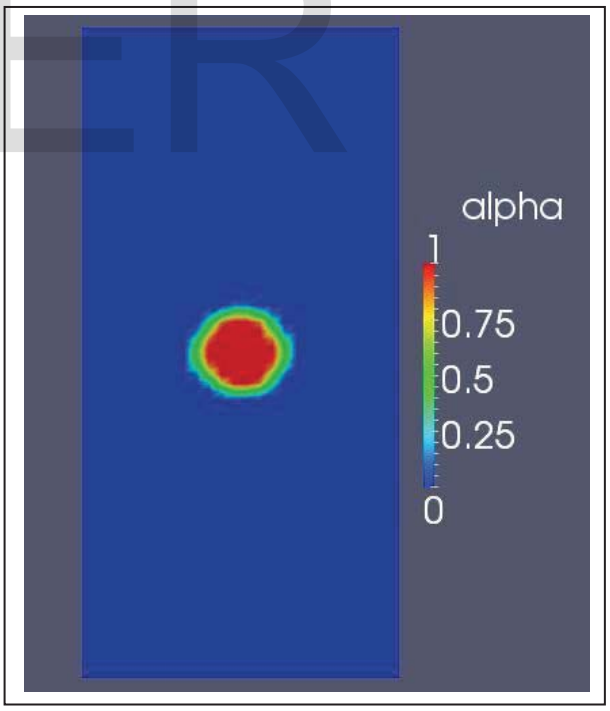

Fig. 7 Void fraction distribution for bubble with D0=0.5mm at time t=0

Fluid properties such as density, kinematic viscosity, specific heat, etc. are specified in the *transportProperties* file. The discretisation schemes and solver settings are provided in the *fvSchemes* and *fvSolution* files in the system directory. Start time, end time, time interval, etc. are given by the *controlDict* file in the *system* directory. Run the case using *bubbleEvapTempFoam* solver and results are viewed in the post processing tool called *paraView.*

VI. Grid Independancy

To check the grid independency, the variation of bubble diameter with time is plotted for various grid sizes for bubble with initial diameter 0.5mm. The grid sizes used were 25×75×25, 50×125×50 and 750×150×75. It was observed that 25×75×25 itself is the stable grid size and is used in modelling the bubble growth phenomena. The grid independency is shown in Fig. 8.

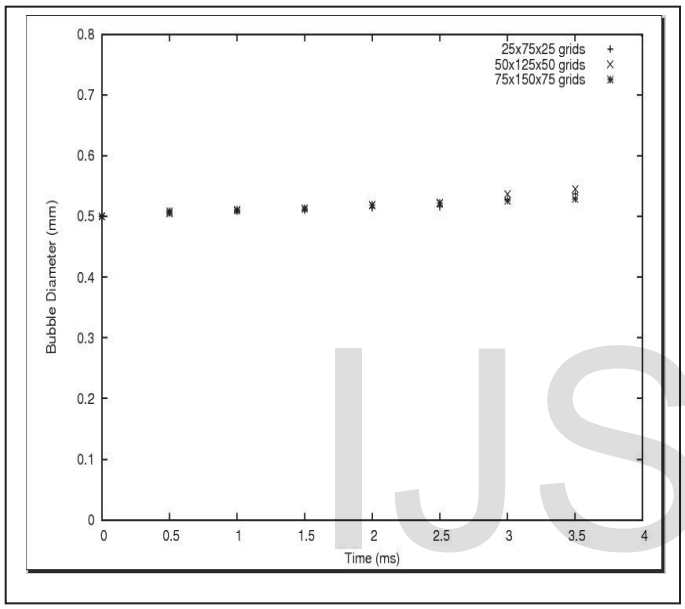

Fig. 8 Test for grid independency

VII. Results and Discussions

Post processing is carried out using the utility *paraView.* The bubble is initially in spherical shape with an initial diameter of 0.5mm. Fig. 9 shows the void fraction distribution across the entire flow domain. With time the shape and diameter of the bubble changes. The bubble moves up due to the fluid velocity and also the lift and drag forces acting on them. It is clearly seen that the shape and diameter of the bubble is changing.

A. Velocity and Temperature Variation

Fig. 10 shows the velocity variation in and around the bubble. The bulk fluid velocity is 0.1m/s. It is seen that the velocity of the vapour portion is always higher. The main reason can be inferred is the buoyancy effect acting on the bubble. The lift and drag forces can also contribute to the difference in velocity of the vapour.

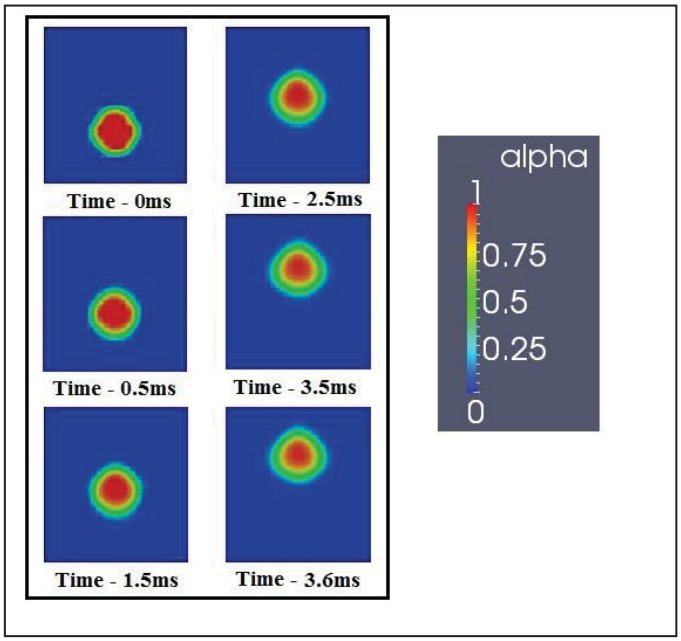

Fig. 9 Void fraction distribution at various times

The temperature variation in and around the bubble is shown in Fig. 11. It can be seen that the temperature at the upper and lower sides of the bubble are different. This might be because the bottom part of the bubble has direct contact to the flowing fluid. So the interaction with the fluid which is at a lower temperature than the vapour phase maintains the bottom part of the bubble at a lower temperature than the top part.

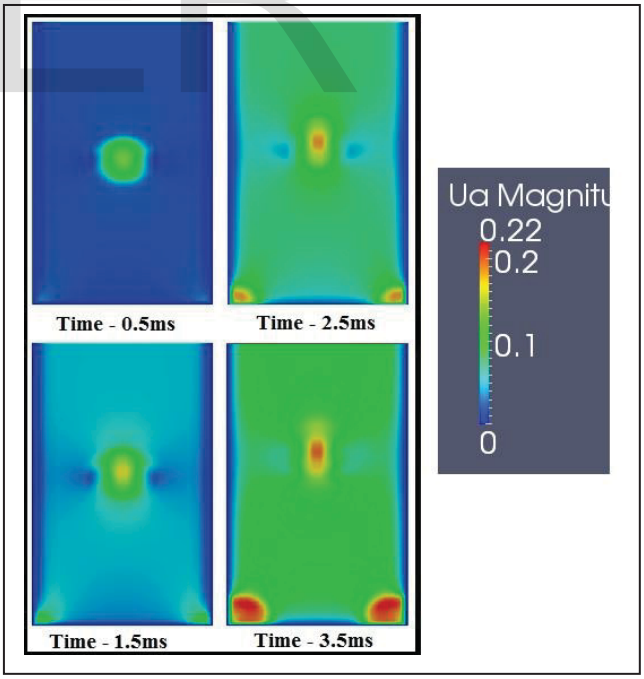

Fig. 10 Velocity distribution in and around the bubble at various times

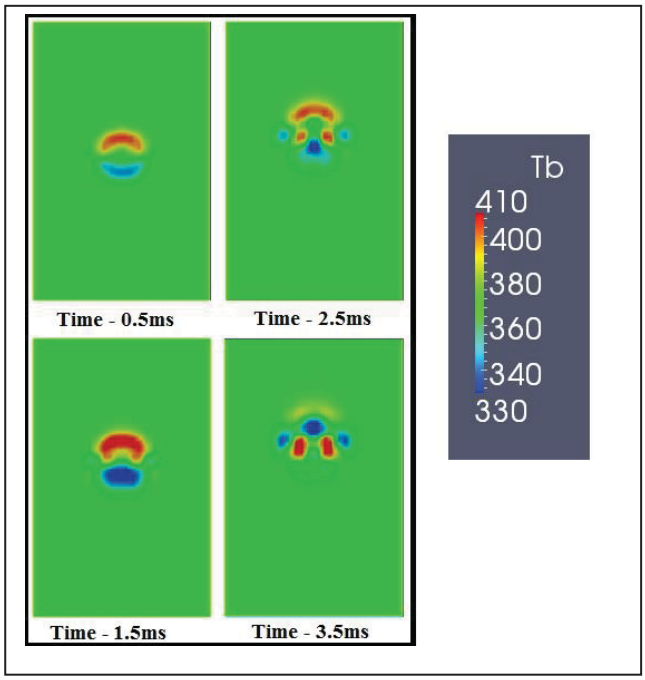

Fig. 11 Temperature distribution in and around the bubble at various times

B. *Variation of Bubble Diameter*

The bubble diameter is found to increase gradually with time. Fig. 12 shows the bubble growth curve. In this the initial diameter for bubble was 0.5mm. The growth curve is then compared with the data from Dhir et al. [7].

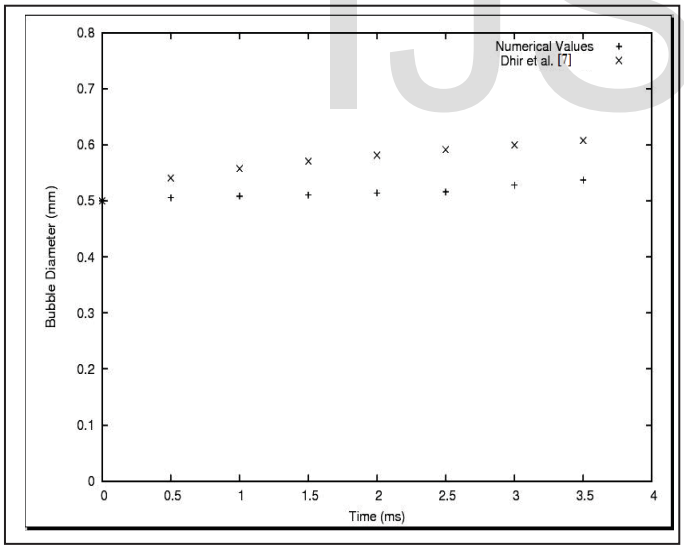

Fig. 12 Variation of bubble diameter with time

Fig. 12 shows that the results vary from values from previous literature. In the present work, only lift and drag are taken as the interfacial forces. Various other forces such as wall lubrication force, turbulent dispersion force, etc. also affect the bubble characteristics (Michta [8]). The force which pulls the bubbles away from the wall is called wall lubrication force. The turbulent dispersion force accounts for the turbulent fluctuations of liquid velocity and the effect it has on the bubbles. For the total heat flux, the evaporative heat flux is only considered. The total heat flux includes quenching and convective heat flux also. The effect of microlayer evaporation is also not included in the work.

C. *Effect of Initial Bubble Diameter*

The modelling is done with different initial vapour bubble diameters. Different diameters used are 0.4mm and 0.5mm. The comparison with different initial bubble diameter is shown in Fig. 13. Both cases are showing same trend in bubble growth.

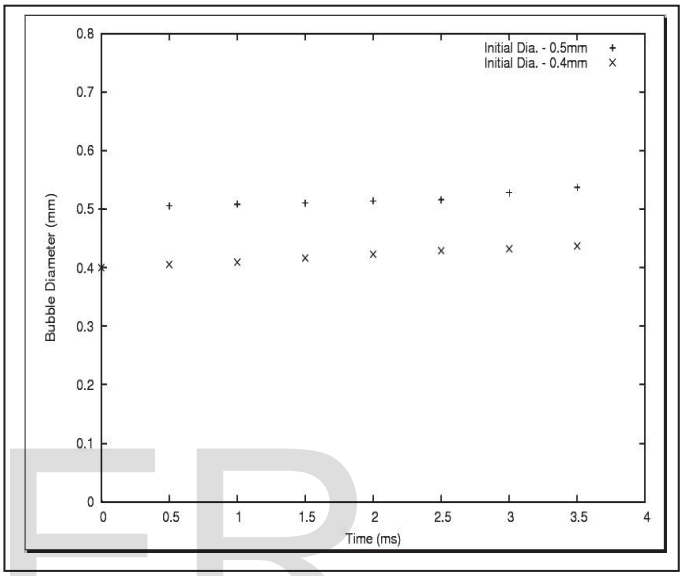

Fig. 13 Effect on initial bubble diameter

VIII. CONCLUSIONS

1) The two-phase modelling of bubble growth in nucleate modelling is done in OpenFOAM by implementing the governing equations to create a new solver.
2) The bubble diameter at different instances is found by using the void fraction distribution and the bubble diameter is plotted against time. The growth of the bubble is compared with data from previous literature and a considerable agreement is found.
3) The upper portion of the bubble, which is facing away from the flow, has higher temperature compared to lower portion. One of the main reasons that can be inferred is the interaction of the flowing fluid with the bubble is more in the lower portion.
4) The velocity contours indicate that velocity of the bubble is always higher than the surrounding fluid velocity. This may be due to the action of drag and lift forces on the bubble. But the main reason is supposed to be the buoyancy force acting on the bubble.

Nomenclature

A_w''	Area of contact (m²)
C_D	Drag coefficient
C_L	Lift coefficient
D_S	Bubble Sauter mean diameter (m)
d_w	Bubble departure diameter (m)
Eo	Eötvös number
f	Detachment frequency (s^{-1})
g	Gravity (m/s²)
i	Specific enthalpy (J/kg)
I	Identity tensor
k	Turbulent kinetic energy (m²/s²)
M	Interfacial forces per unit volume (kg/m²s²)
N''	Nucleation site density (m^{-2})
p	Pressure (Pa)
q_w''	Wall heat flux density (kg/s³)
R	Stress tensor (kg/ms²)
Re_b	Bubble Reynolds number
t	Time (s)
T	Temperature (K or ºC)
U	Velocity (m/s)

Greek Symbols

α	Phase volume fraction
Γ_{gl}	Evaporation rate per unit volume (kg/m³s)
Γ_{lg}	Condensation rate per unit volume (kg/m³s)
ν	Kinematic viscosity (m²/s)
μ	Dynamic viscosity (kg/ms)
μ^*	Dimensionless dynamic viscosity
ρ	Density (kg/m³)

Subscripts

g	gas phase
i	interface
l	liquid phase
m	mixture
max	maximum
sat	saturation
w	wall

Superscripts

D	drag
e	evaporation
L	lift
t	turbulent
T	transpose

References

[1] G Meister, "Vapour bubble growth and recondensation in subooled boiling flow", Nuclear Engineering and Design 54 (1979), pp no. 97-114

[2] R Maurus and T Sattelmayer, "Bubble boundary layer behaviour in subcooled flow boiling", International Journal of Thermal Sciences 45 (2006), pp no. 257-268

[3] D Li and V K Dhir, "Numerical study of single bubble dynamics during flow boiling", Transactions of the ASME 129 (July 2007), pp no. 864-876

[4] R H Khanlou, A Mohammadi and S AJazayeri, "Prediction of bubble lift-off diameter in subcooled flow boiling using AVL fire", Elixir Thermal Engg. 56A (2013), pp no. 13715-13718

[5] A Naber, C Liu and J JFeng, "The nucleation and growth of gas bubbles in a Newtonian fluid: An energetic variational phase field approach", Contemporary Mathematics 466 (2008), pp no. 95-120

[6] R Situ, J Y Tu, G H Yeoh, T Hibiki and G C Park, "Assessment of effect of bubble departure frequency in forced convection subcooled boiling", 16th Australasian Fluid Mechanics Conference, Australia (2-7 December 2007)

[7] V K Dhir, H S Abarajith and D Li, "Bubble dynamics and heat transfer during pool and flow boiling", Heat Transfer Engineering 28(7) (2007), pp no. 608-624

[8] E Michta, "Modeling of subcooled nucleate boiling with OpenFOAM", Master of Science Thesis, Department of Nuclear Reactor Technology, Royal Institute of Technology, Stockholm, Sweden (February 2011), unpublished